Pergamon

Bioorganic & Medicinal Chemistry, Vol. 3, No. 5, pp. 587–604, 1995

0968-0896/95 $9.50 + .00

0968-0896(95)00068-2

Conformational Change Due to Esterification of Hydroxy Groups in Erythromycin A and its Major Metabolite: Analysis of these Derivatives with Different Biological Properties Using NMR and Molecular Dynamics (MD) Data

Patrick Ladam,[a] Josyane Gharbi-Benarous,[a,b] Marcel Delaforge,[a] Marie-Rose Van Calsteren,[c] Christophe K. Jankowski,[c] and Jean-Pierre Girault[a]*

[a]*Université René Descartes, Laboratoire de Chimie et Biochimie Pharmacologiques et Toxicologiques, C.N.R.S. U.R.A. 400, 45 rue des Saints-Pères, F-75270 Paris cedex 06, France*

[b]*UFR Chimie Université Paris 7, Denis Diderot, 2 Place Jussieu, F-75251 Paris cedex 05, France*

[3]*Université De Moncton, Faculté des Etudes Supérieures et de la Recherche, Moncton, Nouveau-Brunswick, Canada E1A 3E9*

Abstract—A conformational study is performed on the acylated erythromycin and erythralosamine derivatives from comparison between experimental results (NMR) and theoretical calculations by Molecular Dynamics (MD) in attempts to correlate their conformations with their abilities to generate cytochrome P450–nitroso metabolite complexes *in vitro*. As the 3'-dimethyl-amino function of the desosamine is metabolized and responsible for the interaction with cytochrome P450, its position, mobility and steric hindrance in the proximity of this functional group are related to its biological properties. The major conformations of the lactone ring were termed **A** (A1, A2, A3) and **B** (B1, B2), and this macrocycle flexibility induced five different orientations **a**, **b**, **c**, **d** and **e** for the desosamine sugar. Conformations **A** and **B** differ in many ways but the major change is the inward folding of the C(3) fragment in **B**. Conformer **a** exhibits an orientation of the desosamine nearly perpendicular to the macrocycle whereas the two units are in the same plane in conformations **c** and **e**. For conformation **b**, the cladinose unit lifts up above the macrocycle. Conformation **d** exhibits a turned-back cladinose. In the erythromycin derivatives esterification at the β position to the $N(CH_3)_2$ group of the desosamine reduces the degree of freedom of the macrocyclic lactone ring which corresponds to conformation **A** only. The desosamine sugar was found to be perpendicular to the macrocycle (**a** conformer) and both sugar groups are parallel to reduce the steric energy. In the erythralosamine derivatives, the macrocycle is always present as conformation **B** with the two conformations **b** and **c** of the sugar rings. The steric parameters favour the **b** conformers in which the amino group is tilted up, while in 3,2'-dibenzoylated stacking aromatic attraction stabilizes the planar **c** conformer. Both isomers are thus shown to adopt well-defined conformations and to be well-adapted for a comparative structure–activity correlation studies. There is a significant relationship between the conformation **b** and the formation of cytochrome P450–nitroso metabolite complexes.

Introduction

Erythromycin A (**1**) is one of the most important members of the macrolide antibiotics.[1] Substantial efforts have been expended in the chemical and biochemical modification of 14-membered macrolides. These were especially directed toward acylation of the hydroxy groups on the lactone ring and on the neutral sugar. Such modifications have been known to improve activity against resistant organisms and improve oral bioavailability[2] of these antibiotics.

2'-Esters of erythromycin and their salts are used because of their favourable pharmacokinetic and pharmaceutical properties. Compared with erythromycin, these substitutes have a lower, incidence of gastrointestinal side effects in patients. In the case of homologous esters, the stabilizing effect of plasma and the concentration dependence varied with the lipophilicity. *In vivo*, 2'-esters are only partially hydrolyzed. It is known that both erythromycin and the unhydrolyzed ester may contribute to the antibacterial activity.

Since hydrogen bonding may be important in biological activity (less freedom for the macrolactone ring and the sugar units and greater hydrophobicity), partial esterification of the hydroxy groups were thought to produce conformational changes in solution, and usually to decrease this activity.[3] Structural changes in the molecule inevitably produce a constant modification in activity.

The effects of macrolides on hepatic metabolic enzymes, especially cytochrome P450, have been studied in order to reduce interference with the metabolism of others drugs.[4] They lead to an induction of cytochrome P450 and to the formation of a stable

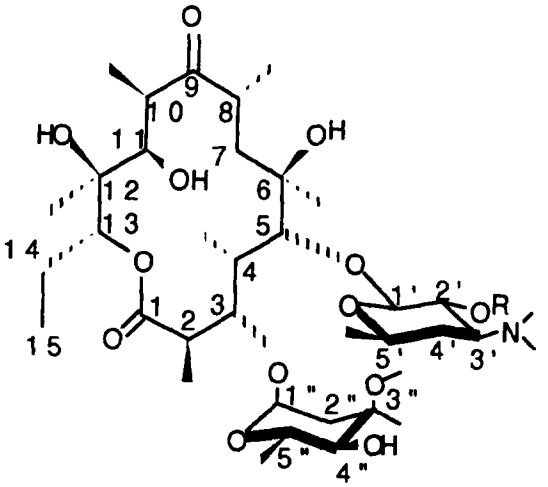

1 Erythromycin R = H
2 2'-propionate erythromycin R = CO-C_3H_7
3 2'-benzoate erythromycin R = CO-C_6H_5

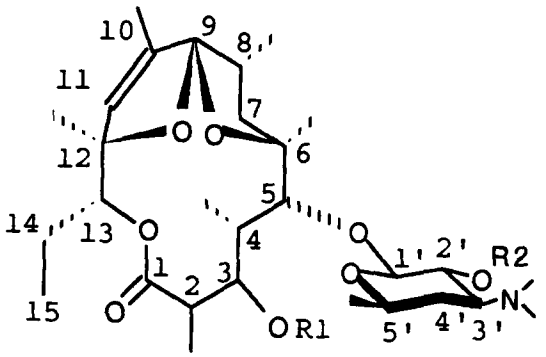

4 Erythralosamine R1 = H R2 = H
5 3-benzoate erythralosamine R1 = CO-C_6H_5 R2 = H
6 2'-benzoate erythralosamine R1 = H R2 = CO-C_6H_5
7 2',3-dibenzoate erythralosamine R1 = R2 = CO-C_6H_5

metabolite–cytochrome P450 complex after oxidation of their dimethylamino function. *In vitro*, 1 has affinity for the cytochrome P450 binding site. It is also able to form significant quantities of P450 metabolite complex[5] (Fig. 1). In previous studies, we investigated erythralosamine (4) a metabolite from erythromycin A (1). A biological study *in vivo*, of the effect of 1 and 4 on hepatic cytochrome P450 has been reported.[6] These studies compare the ability of these molecules to induce cytochrome P450 and to form stable 456 nm absorbing inhibitory cytochrome P450 metabolite complexes. The metabolite of erythromycin, erythralosamine (4), has higher interaction properties whether the studies are performed *in vitro* (Fig. 1) or *in vivo* with the cytochrome P450 system. These important affinities reported with erythralosamine[5,6] could be the cause of the toxic effects and drug interactions observed in animals or humans after treatement with high doses of 1.

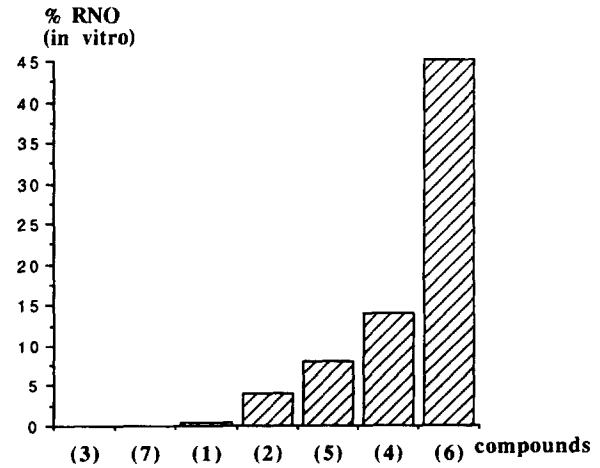

Figure 1. Percentage of cytochrome P450–metabolite complex nitrosoalkyl (% RNO) formed *in vitro* for erythromycin A (1), its metabolite erythralosamine (4) and their derivatives 2–3 and 5–7, respectively. These results are expressed as % cytochrome P450 (RNO) related to the whole concentration of cytochrome P450 (measured as absorbance-difference 450–490 nm of the P450 Fe(II)–CO amounts using 2 μM microsomal cytochrome P450 from dexamethasone treated rats, 30 μM substrate and 500 μM NADPH).

Following oral treatment with macrolide derivatives 1–7, the hepatic cytochrome P450 contents, when compared to control values, showed an increase, except in the case of 2'-benzoate erythromycin (3) and the 2',3-dibenzoate erythralosamine (7) which are not inducers of cytochrome P450 at the dose used. Parts of the induced cytochrome P450 were recovered as nitroso metabolite–cytochrome P450 complexes.

Recognition of the macrolide by the cytochrome P450 active site is not a strict prerequisite for induction and complex formation, but factors such as the presence of an $N(CH_3)_2$ amine function which is oxidized to the corresponding NO group, the accessibility of this amine function which is required for the strong binding of the nitrosoalkane metabolite to the heme, and the hydrophobicity of the molecule, are important during macrolide oxidation *in vitro* or *in vivo*. Induction abilities of macrolides are shown to be also related to their pK_a 7. Esterification at the β position to the $N(CH_3)_2$ group of the desosamine leads to lower pK_a values for the corresponding acido-basic equilibrium. Consequently, better recognition, easier access to the protein active site and significant formation of inhibitory P450–iron-metabolite complexes are expected for these derivatives, but it is not always the case. This is particularly clear in the erythromycin series 1–3. The 2'-propionate erythromycin (2) forms very small amounts of inhibitory complexes and benzoylation in the 2'-position of 1 abolishes induction and formation of cytochrome P450 metabolite complexes for 2'-benzoate erythromycin (3), while 2'-benzoate erythralosamine (6) has higher interaction properties with the cytochrome P450 system than its parent compound 4. However, the benzoate in the 3-position of 4 decreases both induction and complex formation for 3-benzoate erythralosamine (5) and the 2',3'-dibenzoate erythralosamine (7) is fully inactive for both these activities (Fig. 1).

The major aim of the work presented here is to predict the solution conformations of erythromycin derivatives

in an attempt to correlate their conformations with their abilities to generate cytochrome P450–nitroso metabolite complexes *in vitro*. The goal is an important one because formation of these complexes is likely to be responsible for time-dependent inhibition and induction of P450s by erythromycins, phenomena that can lead to life-threatening drug–drug interactions. A major fact of the studies is that the *in vitro* metabolite complex studies were carried out at concentrations of erythromycin and its derivatives that are relevant *in vivo*, and we observed a wide range of extents of complex formation for the series of compounds **1–7** examined. Other facts are the use of several NMR techniques to help establish preferred conformations, and the use of molecular dynamics (MD) as a second tool in this regard. In all cases, the 100 ps time scale seemed adequate for sampling an ensemble of solution conformers.[8]

Results and Discussion

The conformation of **1** and its metabolite **4** in solution, and their motional properties have been studied by NMR spectroscopy and the use of MD simulation.[8] Detailed work using ^{1}H and ^{13}C NMR spectra, ^{13}C relaxation times and also ^{1}H NOE, variable-temperature and variable-solvent experiments proved that a series of derivatives exist in fast equilibrium between different macrolide conformations. Examination of the crystal structures of erythromycin derivatives[9–12] provided models for the different aglycone conformations observed. The major conformations of the lactone ring were termed **A** (A1, A2), **B** (B1, B2) and **S** (named A3), and this macrocycle flexibility induces five different orientations **a**, **b**, **c**, **d** and **e** for the desosamine sugar (Fig. 2). The characteristic parameters of the lactone ring conformations and the different positions of sugar moieties are reported in Table 1. Conformation **A** is based on the crystal structure of erythromycin A,[13] **B** is based on that of erythromycylamine derivative[9] and **S** on that of 9-dihydroerythronolide B derivative.[11] Conformations **A** and **B** differ in many ways but the major change is the inward folding of the C(3) fragment in **B** such that H(3) and H(11) are in spatial proximity. In the same way, conformations **A1** and **A2** differ by the inward folding of H(5) in **A2**. The conformation **S** (A3) is characterized by the C(11)–C(13) segment with a nearly all-*anti* (zig-zag) conformation with the OH(11) and O=C(1) groups close enough to form a hydrogen bridge. Conformational studies of a number of erythromycin A analogues show that these molecules are best described as a blend containing varying proportions of conformations **A** (A1, A2, A3) and/or **B** (B1, B2). Erythromycin underwent an interesting conformational reorganization "**B1** <=> **A1** <=> **A3**" when the conformation in solution of their major metabolite erythralosamine (**4**) as predicted by NMR spectroscopy, was the "folded-C(3)" model **B2**. For erythromycin A (**1**), the major conformations **a**, with an orientation nearly perpendicular to the macrocyclic lactone ring and **c**, with the two units in the same plane, are in fast exchange with a minor conformation **b** with the sugar ring lifted above the macrocycle. This slight participation increases significantly for its metabolite erythralosamine (**4**). There is a significant proportion of an active conformation **B2b** for **4** and an interesting conformational equilibrium in solution for **1** involving a conformation **B1b** which can be related to the interaction with the cytochrome P450 system. It is thought that this conformation could be a potent precursor of erythralosamine conformation **B2b**. Prediction of the solution conformation of these new erythromycin derivatives with such different biological activities would be of great benefit.

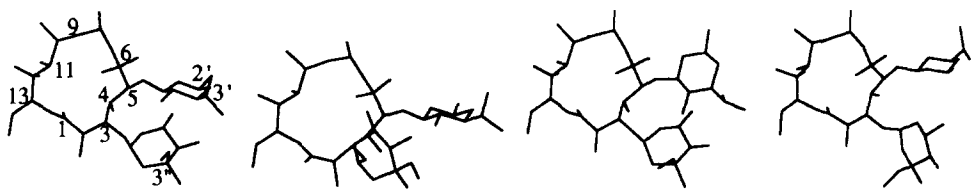

(1) A1a (76%) **(1) B1b** (8%) **(1) A1c** (15%) **(1) A1d** (1%)

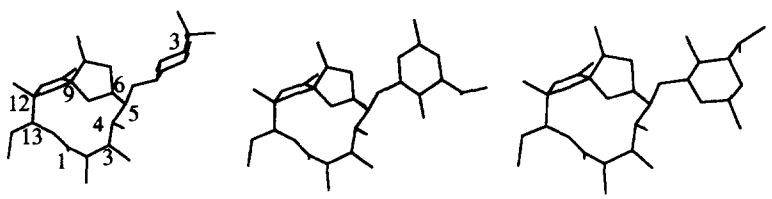

(4) B2b (70%) **(4) B2c** (22.5%) **(4) B2e** (7.5%)

Figure 2. View of the different structures of erythromycin A (**1**): **A1a** (Ep = 67 kcal mol^{-1}), **B1b** (Ep = 69.5 kcal mol^{-1}), **A1c** (Ep = 69 kcal mol^{-1}), **A1d** (Ep = 77 kcal mol^{-1}), and of its metabolite erythralosamine (**4**): **B2b** (Ep = 84 kcal mol^{-1}), **B2c** (Ep = 86 kcal mol^{-1}), **B2e** (Ep = 87 kcal mol^{-1}).

Table 1. The characteristic parameters of the lactone ring conformations and the different positions of sugar moieties: inter-proton distances (p: present, a: absent) and vicinal proton–proton and proton–carbon coupling constants (^3J in Hz) calculated[a] from the different conformations generated by MD

	J_{calc}				
Vicinal pair	A1	A2	A3	B1	B2
J_{HH}					
2-H, 3-H	10.9	10.8	10.8	2.8	7.9
3-H, 4-H	0.8	0.8	0.9	1.7	2
4-H, 5-H	5.3	2.1	6.5	9.1	7.8
7_{ax}-H, 8-H	12.4	12.4	12.5	12.5	12.8
7_{eq}-H, 8-H	1.9	1.6	1.8	1.8	5.1
10-H, 11-H	1.2	1.3	0.8	1.6	(b)
13-H, 14_{ax}-H	11.6	11.6	11.0	11.0	11.3
13-H, 14_{eq}-H	1.6	1.0	1.0	1.0	1.5
J_{CH}					
3-H, 1-C	2	1.9	1.8	5.5	4.1
5-H, 3-C	4.9	5.5	5	3.9	2.7
5-H, 6-C_{Me}	2.6	2.2	2.7	2.1	5.5
13-H, 1-C	5.4	5.3	5.1	5.3	5.6
13-H, 11-C	2.2	2.5	1.5	2.2	6.4
13-H, 15-C_{Me}	2.3	2.3	2.3	2.4	1.9
J_{CH}	a	b	c	d	e
5-H, 1'-C	5-5.5	5.2-5.7	4.3-5.4	5.3	5
5-C, 1'-H	3-4	2-3	4-5	2	6
3-H, 1"-C	4.7	3.8	5	4.8	(c)
3-C, 1"-H	3	3	3.4	5.6	(c)

	Inter-proton distances				
	A1	A2	A3	B1	B2
4-2	p	p	a	p	p
4-2-Me	a	a	a	p	a
5-4-Me	a	a	a	p	p
6-Me-3	a	a	a	a	p
7ax-4-Me	a	p	a	a	a
10-Me-4	a	a	a	a	p
10-Me7ax	a	a	a	a	p
11-4	p	p	p	a	a
11-3	a	a	a	p	a
11-10-Me	a	a	a	a	p
13-12-Me	a	a	a	a	p
15-Me-2-Me	p	a	a	a	a
	a	b	c	d	e
1'-5	p	p	p	p	a
1'-4-Me	p	p	a	p	p
1'-6-Me	a	a	p	a	a
2'-5	a	a	p	a	p
2'-4-Me	a	a	p	a	a
2'-6-Me	a	p	p	a	a
2'-7ax	a	p	a	a	a
2'-10-Me	a	p	a	a	a
5'-4-Me	a	a	a	a	p
5'-6-Me	a	a	p	a	a
5'Me-3	a	a	a	a	p
5'Me-5	a	a	a	p	a
5'Me-7e	a	p	a	a	a
1"-3	p	p	p	p	a
1"-2Me	p	p	p	a	a
1"-5	a	a	a	p	a
2"-2-Me	p	a	p	p	a
3"-OMe-2Me	a	a	a	p	a
3"OMe-4Me	p	p	p	a	a
5"-5	p	p	p	a	a
5"-4Me	a	a	a	p	a
5"-6Me	a	p	a	a	a
5"-Me-6Me	p	a	p	a	a
3"-OMe-1'	p	p	a	a	a
3"-OMe-3'	p	a	a	a	a
3"OMe-5'	a	p	a	a	a
3"OMe-N(Me)$_2$	p	a	a	a	a
5"-1'	p	a	p	a	a
5"-5'	p	a	a	a	a
5"-Me-1'	a	a	p	p	a
5"-Me-3'	a	a	p	p	a
5"-Me-5'	p	a	a	p	a

[a] The calculated $^3J_{HH}$ values would be estimated by an Altona's equation[17] and all $^3J_{CH}$ values by a Karplus type-equation of the form:[18] $^3J_{CH} = 5.7 \cos^2\phi - 0.6 \cos\phi + 0.5$.

[b] $J_{10Me,11H}$ for erythralosamine.

[c] Conformation **e** is only generated by MD for the metabolite 4 without cladinose sugar.

Table 2. ^{1}H NMR chemical shifts (δ_H, ppm) for **1–7** in $CDCl_3$

	1	2	3	4	5	6	7
Lactone							
2	2.87	2.84	2.70	2.72	2.84	2.38	2.62
2-Me	1.18	1.18	1.12	1.10	1.25	0.92	1.04
3	3.99	3.94	3.94	4.26	5.70	4.10	5.60
3-OH	–	–	–	3.25	–	–	–
4	1.97	1.91	1.78	2.24	2.46	2.03	2.26
4-Me	1.10	0.92	0.71	1.03	1.04	0.70	0.72
5	3.56	3.48	3.52	3.41	3.59	3.35	3.51
6-Me	1.46	1.44	1.47	1.40	1.67	1.40	1.60
6-OH	1.51	1.60	1.63	–	–	–	–
7 ax	1.93	1.73	a)	2.31	2.25	2.40	2.40
7 eq	1.74	1.63	a)	1.60	1.66	1.57	1.65
8	2.68	2.66	2.68	2.48	2.56	2.40	2.45
8-Me	1.16	1.17	1.18	0.92	0.94	0.92	0.97
10	3.08	3.07	3.02	–	–	–	–
10-Me	1.14	1.14	1.12	1.85	1.83	1.75	1.78
11	3.82	3.81	3.75	5.50	5.50	5.47	5.45
11-OH	3.95	3.89	3.86	–	–	–	–
12-OH	3.13	3.03	3.07	–	–	–	–
12-Me	1.12	1.13	1.02	1.23	1.25	1.20	1.19
13	5.03	5.05	4.98	4.94	4.98	4.91	4.91
14-ax	1.48	1.49	1.39	1.59	1.62	1.59	1.57
14-eq	1.91	1.91	1.85	1.35	1.35	1.30	1.27
15-Me	0.84	0.84	0.79	0.82	0.85	0.86	0.76
Desosamine							
1'	4.40	4.55	4.69	4.18	4.06	4.38	4.28
2'	3.21	4.78	5.07	3.19	3.18	5.10	5.08
2'-OH	3.45	–	–	3.37		–	–
2'-OR	–	2.33CH_2	8.01(o)	–	8.04(o)	8.05(o)	8.00+8.04
		1.15CH_3	7.42(m)	–	7.41(m)	7.42(m)	7.39+7.42
			7.55(p)	–	7.52(p)	7.53(p)	7.52
3'	2.43	2.62	2.86	2.46	2.41	2.87	2.84
3'$N(Me)_2$	2.29	2.25	2.30	2.29	2.24	2.29	2.25
4'-ax	1.22	1.32	1.40	1.19	1.17	1.33	1.42
4'-eq	1.67	1.73	1.82	1.60	1.61	1.75	1.70
5'	3.48	3.48	3.57	3.48	3.40	3.51	3.49
5'-Me	1.22	1.22	1.27	1.16	1.17	1.21	1.19
Cladinose							
1"	4.88	4.90	4.86	–	–	–	–
2"-ax	1.56	1.58	1.60	–	–	–	–
2"-eq	2.35	2.37	2.36	–	–	–	–
3"-Me	1.23	1.26	1.28	–	–	–	–
3"-OMe	3.31	3.35	3.40	–	–	–	–
4"	3.00	3.02	3.05	–	–	–	–
4"-OH	2.23	2.10	a)	–	–	–	–
5"	3.99	3.98	4.00	–	–	–	–
5"-Me	1.27	1.28	1.30	–	–	–	–

[a]The proton signals were overlapped

NMR Spectroscopy

Chemical shifts and coupling constants are reported in Tables 2–4. These were derived from complete and unambiguous assignments performed on structures **1–7**, using a variety of NMR techniques.

Assignments of ^{1}H and ^{13}C NMR signals. The assignments were made using 1D ^{1}H and ^{13}C (^{1}H decoupled and DEPT-135)[14] spectra, and 2D homonuclear (COSY-60)[15] and heteronuclear (F1 decoupled)[16] shift correlations. Tables 2 and 3 report the ^{1}H and ^{13}C NMR chemical shifts respectively for compounds **1–7** recorded in $CDCl_3$ solution. Analysis of the chemical shift and coupling constant data (Tables 2–4) show that the compounds fell into two distinct groups; Type **A1** (compounds **1–3**) and Type **B2** (compounds **4–7**). Type **A1** compounds have NMR parameters very similar to those for erythromycin A (**1**) and Type **B2** compounds showed close similarities with erythalosamine (**4**) in their ^{1}H and ^{13}C NMR spectra. The assignments were made observing small shift

Table 3. ^{13}C NMR chemical shifts (δ_C, ppm) for 1–7 in $CDCl_3$

	1	2	3	4	5	6	7
Lactone							
1	176.3	175.7	175.8	178.4	176.3	174.6	175.8
2	45.0	44.8	44.8	46.8	48.1	46.7	47.7
2-Me	15.9	15.9	15.9	13.8	15.4	14.1	15.6
3	80.3	79.8	79.7	70.1	73.2	70.8	73.2
4	39.5	39.2	39.3	44.6	45.9	44.7	45.8
4-Me	9.2	9.1	9.4	12.6	12.3	10.9	11.7
5	84.0	83.6	83.2	87.0	87.7	86.7	86.6
6	74.8	74.9	75.2	81.9	83.2	81.7	82.7
6-Me	26.4	26.9	27.3	29.5	29.5	30.8	29.9
7	38.5	38.1	38.1	42.9	43.7	42.7	43.4
8	44.9	45.1	45.2	39.9	40.6	39.9	40.3
8-Me	18.4	18.2	18.1	12.0	12.4	11.8	12.1
9	221.9	222.0	(a)	119.7	120.2	119.4	120.2
10	38.1	37.9	37.7	139.0	139.1	139.3	139.5
10-Me	14.7	12.0	12.0	13.8	13.8	13.8	13.5
11	68.8	68.9	69.0	128.2	128.0	128.4	127.8
12	74.5	74.7	74.5	88.6	89.0	88.6	88.8
12-Me	16.2	16.3	16.2	23.0	23.3	23.3	23.4
13	77.1	76.9	76.8	78.7	78.9	78.8	78.8
14	21.2	21.2	21.1	24.4	24.1	24.4	24.1
15-Me	10.7	10.7	10.7	10.2	10.4	10.2	10.3
Desosamine							
1'	103.3	101.0	101.0	104.5	105.4	102.8	103.0
2'	71.1	71.6	77.2	70.6	70.1	71.5	71.6
2'-OR	–	173.3CO_2	(a)	–	–	(a)	(a)
	–	28CH_2	130 Cq	–	–	128.4Cq	130.5
	–	9.1CH_3	129.8 (o)	–	–	129.7(o)	129.7(o)
	–		128.3 (m)	–	–	128.2(m)	128.2(m)
	–		135.8 (p)	–	–	132.7(p)	132.7(p)
3'	63.3	63.7	63.8	65.4	65.6	63.2	63.1
3'-N(Me)2	40.3	40.7	(a)	40.3	40.4	40.8	40.8
4'	29.2	30.5	30.0	29.1	28.7	32.2	32.2
5'	68.8	68.4	68.9	69.1	69.3	69.1	69.0
5'-Me	21.4	21.2	21.2	21.2	21.2	21.0	21.0
Cladinose							
1"	96.5	96.1	96.1		3-OR		3-OR
					130.6Cq		130.5Cq
2"	35.0	35.0	35.0		129.6(o)		129.6(o)
					128.3(m)		128.3(m)
3"	72.7	72.7	72.9		132.7(p)		132.7(p)
3"-Me	21.4	21.5	21.6				
3"-OMe	49.5	49.4	49.5				
4"	77.9	78.0	77.8				
5"	65.7	65.7	65.8				
5"-Me	18.5	18.6	18.7				

[a]Undetermined because of overlapping ^{13}C resonances.

differences from **1** and **4**. This is substantiated by the fact that the ring appears to be conformationally invariant.

The esterified members of the type **A1** (compounds **2** and **3**) have the same characteristic differences for their ^1H chemical shifts in the erythronolide region H(3)–H(5), H(7) and H(11), methyl groups (4), (6), and Me(10) and the C(1') carbon of the desosamine sugar. The same trends can be seen in a number of other parameters such as ^{13}C chemical shifts and macrolide vicinal coupling constants. The sugar protons of the 2'-esterified compounds **2** and **3** showed a downfield shift and the macrocycle protons, from H(2) to H(7) and from H(10) to H(15), presented distinguishable upfield shifts as they were compared to those of **1**. The ^{13}C NMR chemical shifts of **1**, **2** and **3** were essentially the same except for the C(2') signal in **3** with a significant downfield shift of +6 ppm (Table 3). ^{13}C NMR spectra of both **2** and **3** showed an upfield shift (–2.7 ppm) at C(1') and Me(10) and the downfield at Me(6) and C(4') compared to those of **1** (Fig. S1 of the supplementary material).

Type **B2** compounds undergo differently the changes expected for esterification according to the 3- or 2'-hydroxy group in erythralosamine. In the ^1H NMR spectra of the 2'-esterified compound **6**, the sugar protons were observed downfield and those of macrocycle, from H(2) to H(5) and from H(8) to H(10),

Table 4. Coupling constants ($^3J_{exp}$ in Hz) for **1**–**7** in $CDCl_3$ solution

Vicinal pair	1	2	3	4	5	6	7
J_{HH} (Macrocycle)							
2-Me, 2	7.5	7.0	6.9	7.1	6.5	7.5	7.0
2, 3 [a]	9.4	9.6	10.3	5.6	6.5	7.5	7.0
3, 4	1.5	1.4	2.8	4.0	2.5	2.0	1.5
4, 4-Me	7.4	7.6	7.5	7.1	7.0	7.0	7.0
4, 5 [a]	7.7	7.5	7.5	9.0	10.0	10.0	10.0
7a, 8	11.7	[b]	[b]	13.0	11.0	13.0	12.0
7e, 8	2.5	[b]	[b]	2.0	2.0	2.0	2.0
8, 8-Me	7.1	7.0	7.0	7.0	7.0	7.0	7.0
10, 10-Me	6.9	6.9	6.9	–	–	–	–
10, 11 [c]	1.3	1.8	1.7	*1.5*	*1.5*	*1.5*	*1.5*
13, 14e	2.4	3.1	2.1	3.0	2.0	2.0	2.5
13, 14a	11.0	10.9	10.8	11.5	12.0	11.0	11.0
14, 15-Me	7.4	7.3	7.5	6.5	6.5	6.5	6.5
J_{CH} (Macrocycle)							
5-H, 3-C	5.8	[e]	[e]	2.1	2.2	2.4	<2 [d]
5-H, 6-CMe	3			2.3	3.5	3.4	3.2
J_{HH} (Sugar ring)							
1'a, 2'a	7.2	7.5	7.2	7.1	7.5	7.5	7.5
2'a, 3'a	10.3	10.1	10.5	10.0	10.0	10.0	10.5
3'a, 4'a	12.3	12.1	12.5	12.0	12.0	12.0	12.0
J_{CH} (Glycosidic bond)							
5-H, 1'-C	5.6	[e]	[e]	6.0	5.9	6.3	5.1
5-C, 1'-H	3.2			2.7	2.9	1.9	3.1
3-H, 1"-C	4.3			-	-	-	-
3-C, 1"-H	3.6			-	-	-	-

[a] These $^3J_{HH}$ were indicative of conformational averaging between two or more lactone conformations. In the "folded-in" conformation B1 of the derivative (9*S*)-9-hydroxy-9-deoxoerythromycin A:
$^3J_{2,3}$ = 6.6 Hz and $^3J_{4,5}$ = 5.8 Hz.
[b] Not determined because of overlapping resonances.
[c] $^3J_{10,11}$ for erythromycin derivated and, in italic $^4J_{10Me,11H}$ for erythralosamine derivatives **4**–**7**.
[d] These signals are detected as singlets.
[e] $^3J_{CH}$ could not be estimated as the concentration available is too low.

with distinguishable upfield shifts compared to those for **4**. In contrast, in the ^{1}H NMR spectra of the 3-esterified compound **5**, the erythronolide protons showed a downfield shift at the C(2)–C(6) region when those of desosamine (1', 3', 5') were upfield shifted. These three protons concerned, reveal that the two α faces of the desosamine and the benzoyl rings are opposite to each other in **5**. In contrast with the ^{13}C NMR chemical shifts of **2**, **3** relative to **1**, the ^{13}C NMR spectra of **6** compared to **4**, revealed a downfield of NMe_2 and an upfield shift (–1.7 ppm) of C(1'), C(3') and Me(4), because of steric interaction with the freely rotating benzoyl group (Fig. S2 of the supplementary material). This could be caused likewise by a different orientation of the desosamine sugar, **a** in the 2'-esterified erythromycin **2**, **3** and **b** in the 2'-esterified erythralosamine **6**.

Homonuclear ^{3}J^{1}H-^{1}H *and heteronuclear* ^{3}J^{13}C-^{1}H *coupling constants.* The conformational analysis is based on (i) the values of vicinal $^3J_{HH}$ and $^3J_{CH}$ experimental coupling constants in $CDCl_3$ solution, reported in Table 4 and (ii) the corresponding coupling constants calculated by Altona's equations[17] and Karplus type equation[18] for the C–O–C–H segment from all the minimized structures generated by molecular dynamics (MD) (**A1a** , **A1c**, **B1b** and **B2b**, see further, Table 5).

A trend in the tabulated $^3J_{HH}$ and $^3J_{CH}$ values, listed in Table 4 for compounds **1**–**7**, can be seen as the conformational blend alters from being predominantly type **A** or **B** with the desosamine sugar being nearly perpendicular to the macrocyclic lactone ring, (**a**) orientation or perpendicular lifted up (**b**) type or mainly coplanar (**c**) type (Figs 3 and 4).

Averaging is required to correctly predict properties for population of low-energy computer models distributed over *P* conformational states (Table 5). The relative population of the *i* th conformational state, P_i with energy E_i, is dictated by the Boltzmann distribution,

$$P_i = \exp(-E_i / kT) / \sum \exp(-E_i / kT). \quad (1)$$

By using the fractional population for each conformational microstate, the average coupling constant can be computed from:

$$^3J_{(HH)} = \sum P_i * {}^3J_{i(HH)}. \quad (2)$$

The coupling constants ^3J(HC) across the glycosidic bond that accommodates conformational flexibility

Table 5. Energy, statistical participation and torsion angles computed for **1–7** by MD (calculated[a] coupling constants)

Compound & Conformation	E kcal mol^{-1}	%	Ψ_1	Ψ_2	Ψ_3 (b)	Ψ_4 (b)	H_2H_3	H_4H_5	H_5Me_6	$H_{13}C_1$	$H_{13}H_{14}$ (c)
(1) **A1a**[d]	67.3	76	17.1(5.1)	38.7(3.5)	27.7(4.4)	43.1(3.1)	161.8(10.6)	134.1(6.9)	44.7	-10.1	-175.0
(1) **B1b**[d]	69.5	8	9.9(5.4)	53.7(2.1)	38.9(3.5)	53.3(2.2)	101.2(1.6)	162.4(10.6)	54.6	13.8	-173.9
(1) **A1c**[d]	68.9	15	-21.1(4.9)	3.6(5.6)	19.4(5.0)	35.2(3.8)	166.2(10.9)	141.9(8.2)	39.8	-12.2	-175.1
Average values	67.7	-	15	37	27	42	161	136	45	-10	-175
(Amplitude)	4	-	44	53	24	19	69	30	18	36	2
(2) **A1a**[d]	74.3	75	11.7(5.4)	43.9(3.0)	29.0(4.3)	45.0(2.9)	161.6(10.4)	131.6(6.2)	45.5	-9.4	-175.1
(2) **B1b**[d]	76.9	5	16.4(5.2)	51.8(2.3)	35.2(3.8)	43.6(3.0)	114.5(3.5)	145.3(8.3)	52.9	12.2	-174.4
(2) **A1c**[d]	75.3	20	-34.8(3.8)	20.5(4.9)	10.0(5.4)	28.6(4.3)	170.2(11.1)	149.9(9.1)	34.2	-21.0	-174.0
(3) **A1a**[d]	133.0	100	13.4(5.3)	42.1(3.2)	28.3(4.4)	43.7(3.0)	164.1(10.7)	132.3(6.3)	44.7	-10.1	-175.1
(4) B2b	86.3	9	-12.8(5.3)	54.1(2.1)	-	-	142.4(8.3)	167.8(10.9)	-8.1	17.4	-90.8
(4) **B2b**	84.4	61	-12.6(5.3)	57.5(1.8)	-	-	149.8(9.4)	166.3(10.8)	-7.9	1.5	-179.9
(4) B2c	87.5	25	-30.1(4.3)	-27.4(4.5)	-	-	142.9(8.4)	167.2(10.8)	-7.1	17.3	-90.7
(4) **B2c**	85.6	20	-30.0(4.3)	-23.8(4.7)	-	-	149.9(9.4)	166.7(10.8)	-7.6	1.5	-179.9
(4) **B2e**	86.5	7.5	-2.8(5.6)	165.6(6.4)	-	-	151.0(9.6)	164.1(10.7)	-7.3	1.5	-179.9
Average values	85	-	-15	54	-	-	142	166	-8	3	-176
(Amplitude)	5	-	28	200	-	-	13	7	6	20	90
(5) **B2b**	136.7	52	-10.6(5.4)	52.4(2.3)	-29.4(4.3)	- 175.3(6.7)	152.5(9.7)	169.0(10.9)	-12.0	-2.9	178.9
(5) **B2c**	136.8	48	-27.5(4.4)	-25.2(4.6)	-30.7(4.1)	- 165.0(6.4)	152.8(9.8)	164.3(10.7)	-7.4	-2.1	179.1
Average values	137.4	-	-11	48	-21	-171.4	150.1	167	-10	0.3	179
(Amplitude)	3	-	42	90	47	45	18	18	11	15	1
(6) B2b	135.1	11	-3.5(5.6)	61.8(1.5)	80.9	-	145.2(8.8)	166.6(10.8)	-8.3	14.9	-90.6
(6) **B2b**	133.2	75	-7.0(5.5)	63.0(1.4)	-173.4	-	150.5(9.5)	167.0(10.8)	-9.1	1.2	-179.9
(6) B2c	137.0	2	-40.7(3.3)	-25.1(4.6)	-171.3	-	149.1(9.3)	161.3(10.5)	-4.0	9.8	-90.1
(6) **B2c**	135.0	12	-40.8(3.3)	-23.6(4.7)	-170.0	-	152.8(9.8)	161.5(10.5)	-4.5	-0.2	-179
average values	134.3		-21	48		-	149	166	-8	2.4	-171
(Amplitude)	6		44	96		-	13	10	12	22	91
(7) **B2b**	183.9	15	-4.4(5.6)	61.6(1.5)	-28.8(4.3)	- 176.0(6.8)	149.8(9.4)	167.2(10.9)	-10.3	-1.5	-179.9
(7) **B2c**	182.1	85	-39.9(3.4)	-13.7(5.3)	-12.5(5.3)	161.1(6.2)	146.3(8.9)	165.7(10.8)	-6.2	-2.5	-179.7
Average values	183.9	-	-35	46	-29	-174	151	164	-8.4	-2.0	-178.9
(Amplitude)	5	-	42	91	40	55	14	17	12	8	2

[a]The calculated $^3J_{HH}$ values for the MD conformations would be calculated by Altona's equations[17] and all $^3J_{CH}$ values by a Karplus type-equation:[18] $^3J_{CH} = 5.7 \cos^2\phi - 0.6 \cos\phi + 0.5$.

[b]Ψ_3 = H3C3–O3Co; Ψ_4 = C3O3–CoCbz for **5** and **7** and Ψ_3 = H3C3–O3H for **6**.

[c]The amplitude of movement of the ethyl group (C14-C15) leads to two positions, parallel ($\phi_{13,14} \approx 180°$, $^3J = 11.3$ Hz) and perpendicular ($\phi 13,14 \approx 90°$, $^3J = 0.7$ Hz) to the macrocycle, only for the (**4**) and (**6**) conformations **b** and **c**.

[d]The calculated $^3J_{HH}$ values of **A1a**, **A1c**, **B1b** are equivalent for **1**, **2** and **3**

were also used and combined with results from computerized molecular dynamics.

$$^3J_{(HC)} = \sum P_i * {}^3J_{i\,(HC)}. \qquad (3)$$

The rotation of the C(3)–C(5) fragment is evident by the observation of the changing values of $^3J_{2,3}$ and $^3J_{4,5}$ driven by the different C(2') and C(3) substituents.

The torsion angles of the aglycone in **2** and **3** and **5–7** agree well with those in **1** and **4**, the **A1** and **B2** models respectively, within the C(6)–C(9)–C(1) region of the molecule, but slightly differ in the C(2)–C(5) region.

The conformation of macrolactone **1–3** places the 3- and 5-oxygen in a *syn*-periplanar relationship which then requires that the orientations of H(4) and H(5) be $\phi = 130°–140°$ and $J_{4,5} \approx 7–8$ Hz, which correspond to a transoïdal angle in an eclipsed Newman projection. However, in the erythralosamine series **4–7** the magnitude of $J_{4,5}$ is markedly increased to 10 Hz and no stabilizing hydrogen bonds occur.[8] In addition, the bulk of the translactonization will destabilize the 3- and 5-oxygen periplanar conformation and require some reorganization to minimize this interaction. A rotation of the 4–5 bond effectively increases the dihedral angle between H(4) and H(5) beyond the 160°–170° range, thereby increasing the $J_{4,5}$. The reorganization appears to be limited to the C(3)–C(5) portion of the aglycone ring since $J_{2,3}$ is the only other coupling constant affected. The conformational equilibrium is such that $J_{2,3}$ decreases while $J_{4,5}$ increases in going from one limiting conformation **A** to another **B**. The coupling constants (Table 5) were calculated from the corresponding dihedral angles of each conformer generated by molecular dynamics. They are in good agreement with those obtained from NMR spectra. The small difference for $J_{2,3}$ experimental in the

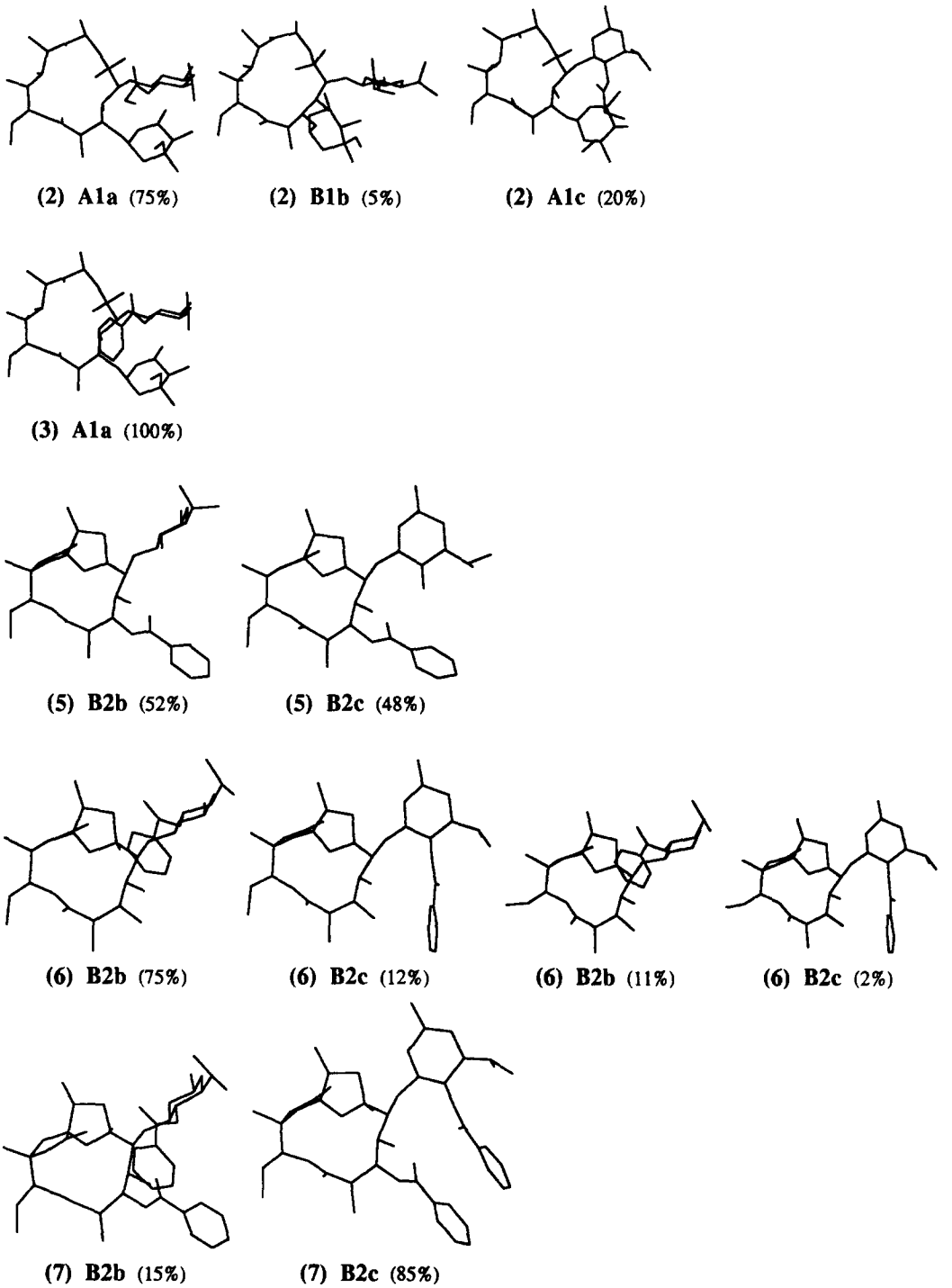

Figure 3. View of the different structures generated by a systematic conformational search for the acylated derivatives of erythromycin A **2** and **3** and of its metabolite erythralosamine **5–7**: (**2**): **A1a** (Ep = 74.3 kcal mol^{-1}), **B1b** (Ep = 76.9 kcal mol^{-1}), **A1c** (Ep = 75.3 kcal mol^{-1}); (**3**): **A1a** (Ep = 133.0 kcal mol^{-1}); (**5**): **B2b** (Ep = 136.7 kcal mol^{-1}), **B2c** (Ep = 136.8 kcal mol^{-1}); (**6**): with the ethyl group in a parallel position **B2b** (Ep = 133.2 kcal mol^{-1}), **B2c** (Ep = 135.0 kcal mol^{-1}) and with the ethyl group in a perpendicular position **B2b** (Ep = 135.0 kcal mol^{-1}), **B2c** (Ep = 137.0 kcal mol^{-1}); (**7**): **B2b** (Ep = 183.9 kcal mol^{-1}), **B2c** (Ep = 182.1 kcal mol^{-1}).

erythromycin series, between **1** and **2**, **3** is attributed to a slight variation in the conformational averaging. This would result from the presence in solution of the minor conformation that affects conformer **A1a** ($J_{2,3}$ = 10.6 Hz) in this region as is the case in the "folded-in" conformation model **B1b** ($J_{2,3}$ = 1.6 Hz).

In the derivatives **4–7**, besides the loss of cladinose sugar, the macrocycle unit is strongly modified by two cyclizations and this particular conformation of the macrocycle is denoted **B2**. Strong distortions can thus be observed compared to erythromycin mainly for the C(3)–C(5) region. The 2–2.3 Hz measred coupling constant for the H(5)C(5)–C(4)C(3) dihedral angle is significantly lowered compared to the values observed for the other **A1** compounds (in the range of 5 to 6 Hz). For erythromycin, its minor conformer **B1b** exhibits such a calculated value (3.7 Hz) and it is thought that

this conformation could be a potent precursor of erythralosamine conformation **B2b**.

The measurement of heteronuclear long-range ^3J ^{13}C–^1H coupling constants (Table 4) combined with studies by molecular dynamics (Table 5) was also useful to identify the positions and mobility of the sugar moieties with respect to the erythronolide (Fig. 4). It is of particular interest since it could be related to the different biological properties of these molecules.[8] Values of the coupling constants obtained from selective 2D INEPT[19] are given in Table 4 for the glycosidic bonds.

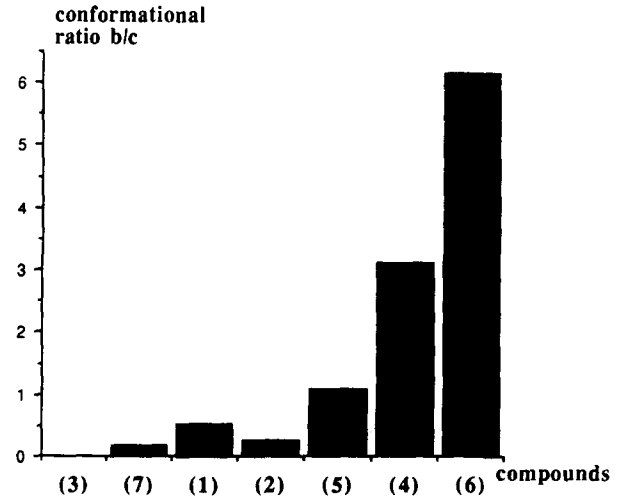

Figure 4. Percentage of the desosamine conformation **b** related to compounds in the order of Figure 1, according to the amounts of cytochrome P450–metabolite complex (% RNO) formed *in vitro*.

In a previous study[8] on **1** and **4**, MD has given five common families of desosamine sugar, **a**, **b**, **c**, **d** and **e**, with different values for Ψ_1, Ψ_2, Ψ_3, Ψ_4 (Figs 3 and 4). Conformer **a** ($J_{\Psi 2} \approx 3.5$ Hz) exhibits an orientation of the desosamine sugar nearly perpendicular to the macrocycle whereas the different ring units seem to be in the same plane in conformations **c** ($J_{\Psi 2} \approx 5$ Hz) and **e** ($J_{\Psi 2} \approx 6$ Hz). For conformation **b** ($J_{\Psi 2} \approx 2$ Hz), the cladinose unit lifts up above the macrocycle. The conformation **d** ($J_{\Psi 2} \approx 3$ Hz) of higher energy exhibits a turned-back cladinose and it is only observed in the case of erythromycin. Experimental values (Table 4) are discussed with regard to the calculated values in these different conformers (Table 5) from the lowest structures in energy (in a range of 2 or 3 kcal mol^{-1}).

The presence of the **b** conformation should increase the coupling constant corresponding to Ψ_1 and at the same time, decrease that of Ψ_2, but the participation of the other conformation **c** increases the value of $J_{\Psi 2}$ and decreases that of $J_{\Psi 1}$. The observed values for $J_{\Psi 1}$ and $J_{\Psi 2}$ in the Table 4 should include a larger participation of conformer **b** for **6** and predominantly for the other erythralosamine derivatives (**5** and **7**), a conformation **b** in equilibrium with the model **c**, as it is noted by the MD study describing an average of **b** and **c** (Fig. 4).

Nuclear Overhauser enhancement (NOE) experiments. 2D Phase-sensitive ^1H NOESY experiments in $CDCl_3$ were performed using a time-proportional phase-increment method[20] and different mixing time (τ_m). ^1H NOE difference experiments in $CDCl_3$ were used to confirm that the pattern of NOEs involving the **2** and **3** protons is similar to that found in erythromycin A.[8,9] The phase sensitive NOESY spectra of **4–7** are acquired with τ_m = 400, 600 and 800 ms and the values are collected in Table 6. Both coupling constants and NOE can give indications about ring conformation. The possible conformational flexibility of the sugar ring in the five orientations complicates the analysis of the NOESY spectra. The observed inter-residue NOE values are compared with spatial proximity distances computed from the low-energy conformers **5–7** having sugars in **b** or **c** positions (Table 7).

Table 6 includes some interesting intra-residue NOEs. Strong NOEs were observed between Me(8) and Me(10) and between Me(10) and H(11) in **4–7**, establishing the erythronolide conformation **B2** and the stereochemistry on the ethylenic system 10Z,9R. Differences from macrolides were observed for some NOEs, particularly those from H(11) such as [11]4 expected for models **A** while [11]3 and [11]10-Me are only observed for conformers **B1** and **B2**, respectively. The very small NOE [11]3 due to the minor conformer **B1**, is only observed for erythromycin A, for which this minor conformer **B1** is in equilibrium with the major one **A1**. This is confirmed by the presence only for **1**, of the small NOE [4Me]5 which appears only in the **B** models. In the same way, the large NOEs [10Me]4, [10Me]7ax, [11]10Me, [6Me]3 observed for erythralosamine derivatives as large as NOE [14e]11, characterize and confirm the **B2** conformation for **4–7**. Moreover for **4–7**, the particular conformation **b** of the desosamine sugar rejected close up towards the macrocycle is confirmed by the characteristic spatial proximity between H(2') and Me(6), H(7a) and Me(10). In molecules **4–7**, the desosamine sugar makes a "**b** <=> **c**" interconversion. Three desosamine–lactone spatial proximities (Table 7), particularly those from Me(6) are characteristic and correspond to an interaction between the macrocycle and the conformation **c** nearly coplanar to the lactone ring, [1']6Me, [2']6Me and [5']6Me. The corresponding NOEs between Me(6) and H(2') and (5') are found to be large in the derivative **7**. Most resonances overlap with other signals, making it difficult to measure the effects on other specific resonances.

It appeared that the OHs were H-bonded in erythromycin A (**1**): the OH(6) and the OH(11) to 9-ketone, the OH(4") to the OCH_3(3"), and the OH(12) to the OH(11). In the 3-benzoylated derivative **5**, a new

Table 6. Qualitative nuclear Overhauser enhancement data for **1–7** in $CDCl_3$ solution

	NOE[a]				
Hobserved	1-3	4	5	6	7
2-Me	2(l)	2(l)	2(l)	2(l)	2(l)
3	2(s),2Me(s)	2(m)	2(m),2Me(m)	2(m),2Me(m)	2(m),2Me(s)
4	2(m),3(m)	2(m),2Me(s),3(m)	2(l),3(m)	2(l),3(m),2Me(m)	2(l),3(m)
4-Me	2(m)	2(m),3(s)	3(s),4(l)	2(m),4(l)	2(s),3(s),4(l)
5	3(m),4(s),4Me(s)	3(m),4Me(l)	3(l),4(m),4Me(m)	3(l),4(m),4Me(l)	3(l),4(s),4Me(m)
6-Me	5(m)	3(l),5(l)	3(l),5(l)	3(l),5(l)	3(l),5(l)
7-ax		5(s)			
7-eq	6Me(s)	5(s)	7a(l)	7a(l),6Me(l)	7a(l)
8	6Me(l),7e(s)	6Me(l),7e(m)	6Me(l),7e(l)	6Me(l),7e(l)	6Me(l),7a(s),7e(l)
8-Me	7e(s)	7a(m),7e(m)	7a(m),8(l)	7a(m),7e(m),8(l)	7a(m),7e(s),8(l)
10-Me	8(s),10(l)	4(l),4Me(s),7a(l),8Me(l)	4(l),7a(l),8Me(m)	4(m),7a(l),4Me(s),8Me(l)	4(l),7a(l),8(s),8Me(l)
11	3(s)*,4(m),7a(s)	7(m),10Me(l)	2(s),10Me(l),8Me(s)	10Me(l)	8Me(s),10Me(l)
12-Me	11(m)	11(l)	11(m)	11(m)	11(l)
13	11(m)	4(m),11(s),12Me(l)	12Me(m)	12Me(l)	
14-ax	12Me(m),13(s)	12Me(m),13(l)	12Me(m),13(m)	12Me(l),13(l)	12Me(l),13(l)
14-eq	13(s)	11(m),13(m)	11(l)12Me(s)13(s)	11(m)	11(l),13(l)
15-Me	13(m),14(m)	11(s),13(l),14(l)	11(s),13(l),14(m)	2Me(m)11(s)13(l),14(m)	2Me(s),11(s),13(l),14(l)
1'	4Me(s),5(m)	5(l),4Me(m)	5(l),4Me(m)	5(l),4Me(l)	5(l),4Me(m)
2'		6Me(s),7a(s),10Me(s)	7a(m)§	6Me(m)7a(s)10Me(m)	7a(s),10Me(s)
2'-OH		4Me(s)	1'(s)		
3'			1'(l)	1'(l),2'(s)	1'(l),2'(m)
3'-N$(Me)_2$		2'OH(m)	2'(l),3'(l)	Hortho(m),2'(l),3'(l)	Hortho(s),2'(l),3'(l)
4'-ax			2'(m),N$(Me)_2$(m)	2'(m),N$(Me)_2$(m)	2'(m),N$(Me)_2$(m)
4'-eq			3'(m),4'a(l)	3'(m),4'a(l)	3'(m),4'a(l)
5'			1'(l),3'(l),4'e(m)	1'(l),3'(l),4'e(m)	1'(l),3'(l),4'e(m)
5'-Me		7e(m),5(s)	7e(s),5'(l),4'e(l)	5'(l),4'(m)7e(m)	5'(l),4'(m)
Bz-Ho			2Me(m),4Me(m)	4Me(l)10Me(m)	2Me(m)4Me(l)10Me(s)
Bz-Hm			Bz-Ho(l)	Bz-Ho(l)	
Bz-Hp			Bz-Hm(l)	Bz-Hm(l)	

[a] l = large, > 5%, m = medium, > 1%, < 5%, s = small, < 1%.
NOEs involving the **2** and **3** protons are similar to those found in erythromycin A (**1**).[8,9]
*Not observed for **3**.

Table 7. Summary of inter-proton distances (2–3.5 Å, p: present, a: absent) from minimized structures derived from MD at 300 K

	(5) b	(5) c	(6) b	(6) c	(7) b	(7) c
7-eq-6-Me	a	p	p	p	a	p
1'-4-Me	p	a	p	a	p	a
1'-6-Me	a	p	a	p	a	p
1'-7ax	a	p	a	p	a	p
1'-7eq	a	p	a	p	a	p
2'-7ax	p	a	p	a	p	a
2'-4-Me	a	p	a	p	a	p
5'-7eq	a	p	a	a	a	p
5'-Me-6-Me	p	a	p	a	p	a
5'-Me-7e	p	a	a	a	a	a
Hortho-2-Me	p	p	a	a	p	p
Hortho-4-Me	p	p	p	a	p	a
Hortho-5	a	a	a	p	a	p
Hortho-10Me	a	a	p	a	p	a
Hortho-N(Me)	a	a	p	a	p	p

intramolecular hydrogen bond (involving the desosamine sugar) appear in some generated structures, (2')OH–O(5). Perhaps this new hydrogen bond formed, lowers the barrier enough to favour interconversion "**b** <=> **c**" in the compound **5** with respect to **4**. The alkyl chains of the esters may form an intramolecular hydrophobic interaction with the non-polar surface of the molecule. The benzoyl group at position 3 (**5** and **7**) has its H_{ortho} in spatial proximity with Me(2) and Me(4). This last [4Me]H_{ortho} NOE is found again in **6** with a benzoyl group at 2'-position, but only observed in the conformation **6b**. The 2'-benzoate erythralosamine derivatives **6b** and **7b** present characteristic inter-residue distances similar for [10Me]H_{ortho} and [NMe_2]H_{ortho} in particular producing specific NOEs. In contrast, the inter-residue [5]H_{ortho} NOE is only observed in the **6c** and **7c** conformers. The presence of a benzoyl group at position 3 in **5** and/or 2' in **6** and **7** is characterized in (i) conformations **5–7 b** by the NOEs [1']4Me, [2']7a, [5'Me]6Me and (ii) conformation **5–7 c** by the NOEs [1']6Me, [1']7, [2']4Me.

^{13}C longitudinal relaxation times (T_1). Information about the structural flexibility of these compounds can be experimentally obtained from the T_1 relaxation times of the carbon resonances. The NT_1 values (N = number of attached protons, T_1 = longitudinal relaxation time) correlate directly with the molecular mobility. This is due to the fact that the ^{13}C relaxation of these carbons is mainly dominated by the single relaxation mechanism, that is, ^{13}C–^1H dipolar interaction with directly bonded hydrogens.[21]

The values of NT_1's measured by inversion–recovery experiments are reported in Table 8. These data provide information about rotational motion of the backbone of the derivative molecules and about the internal rotations of the sugar units. All the carbons gave very similar NT_1 values, indicating rigidity of the backbone. For example, erythralosamine (**4**) and the derivatives **5–7** produce differences in their ability to form stable cytochrome P450–metabolite complexes (Fig. 1): the dibenzoate **7** does not form an inhibitory P450–metabolite complex and the 3-benzoate **5** just a little. Thus, T_1 values for $N(Me)_2$ compared to **4** were indicative of sterically hindered rotation in **7**, and also in **5**. So, the $\Delta^{13}CT_1$ evaluated between the erythralosamine product **4** and the **5**, **7** derivatives are (–10%) for the $N(Me)_2$ group which has consequently lost some of its mobility. An inter-unit NOE is observed between H_{ortho} of the benzoyl substituent and the dimethylamino group of the desosamine sugar for **7**. By contrast the 2'-benzoate derivative **6**, has higher interaction properties with the cytochrome P450 system and when one compares the ^{13}C NT_1 values from **6** to **4** given in Table 8, they show by the $\Delta^{13}CT_1$ of $N(Me)_2$ = +32%, that in derivative **6**, the desosamine group is more free to rotate.

For the methyl carbons 2, 4 and 15, the NT_1's are larger in erythralosamine (**4**) than in the derivatives **5–7**. This shows that these methyls are less mobile than in the parent compound and are closer to the benzoyl substituent in the isomers **5–7**. This perhaps confirms the position and the orientation of the benzoyl substituent in the isomers **5–7**, shown by inter-units' NOEs [2Me]H_{ortho}, [4Me]H_{ortho}, [10Me]H_{ortho}. This last NOE is not observed in the **5** isomer, therefore, the $\Delta^{13}C$ T_1 of 10Me evaluated between **5** and **4** is +21% instead of –14% and –3% for **6** and **7** with respect to **4**.

Table 8. Experimental ^{13}C and ^1H NMR relaxation times ($CDCl_3$ solution) for the methyl groups in **1–7**

	1		**2**		**3**[a]		**4**		**5**		**6**		**7**	
	$^{13}CNT1$,s	$^1HT1$,s	$^{13}CNT1$,s	$^1HT1$,s	$^{13}CNT1$,s	$^1HT1$,s	$^{13}CNT1$,s	$^1HT1$,s	$^{13}CNT1$,s	$^1HT1$,s	$^{13}CNT1$,s	$^1HT1$,s	$^{13}CNT1$,s	$^1HT1$,s
Lactone														
2-Me	0.78	0.20	0.75	0.28	0.23		1.62	0.32	1.11	0.28	1.35	0.38	0.87	0.26
4-Me	1.80	0.33	2.82	0.29	0.26		1.47	0.30	1.08	0.24	1.32	0.30	0.78	0.23
6-Me	1.89	0.30	1.59	0.27	0.30		2.85	0.39	5.55	0.40	2.94	0.42	3.09	0.38
8-Me	1.56	0.29	1.56		0.31		3.33	0.45	1.05	0.45	2.40	0.41	3.66	0.43
10-Me	2.10	0.38	3.21	0.35	0.35		4.20	0.47	5.07	0.51	3.60	0.50	4.08	0.47
12-Me	1.47	0.28	1.47	0.35	0.29		1.44	0.31	1.20	0.30	1.41	0.32	2.43	0.30
15-Me	3.00	0.52	3.06	0.42	0.51		3.93	0.53	2.34	0.53	2.07	0.59	1.80	0.52
Desosamine														
1'	0.80	0.32	0.43	0.35	0.32		0.65	0.43	0.60	0.38	0.57	0.43	0.64	0.39
2'	0.52	0.64	0.41	0.78	0.80		0.58	0.69	0.51	0.56	0.62	0.83	0.54	0.73
3'	0.63	0.35	0.44	0.47			0.61	0.39	0.62	0.34	0.56	0.52	0.55	0.48
3'N (Me)2	1.80	0.35	2.10	0.41			1.95	0.37	1.77	0.35	2.58	0.44	1.77	0.40
4'	0.22	0.20	0.25		0.25		0.33	0.23	0.37	0.27	0.29	0.37	(b)	0.30
5'	0.69	0.48	0.50	0.38	0.27		0.64	0.55	0.69	0.52	0.61	0.51	0.38	0.48
5'-Me	2.19	0.42	(b)		0.73		2.46	0.39	2.49	0.40	2.10	0.44	(b)	0.43
Cladinose														
3"-Me	1.98	0.38	1.86		0.42		–	–	–	–	–	–	–	–
3"-OMe	3.39	0.59	3.63	0.61	0.57		–	–	–	–	–	–	–	–
5"-Me	2.01	0.38	2.19	0.32	0.41		–	–	–	–	–	–	–	–

^{13}C T_1 and ^1H T_1: experimental results in $CDCl_3$ solution at ambient temperature; T_1 = spin-lattice relaxation time. N = number of protons on each carbon. The average error of the T_1 determinations are estimated to be 0.03 s for all compounds.

[a] ^{13}C T_1 could not be estimated as there is not enough product.

[b] ^{13}C T_1 could not be estimated because of overlapping signals.

The $^{13}CT_1$ value of **5** relative to that of erythralosamine (**4**) is increased by +95% for 6Me. The benzoyl group, particularly in the 3-benzoate derivative **5** compensates the loss of the cladinose sugar and the orientation of the desosamine and aromatic rings with respect to one another is almost the same for erythromycin and the **5** substance (Fig. 4).

Molecular dynamics. The MD simulations were carried out using the 'DISCOVER' program of Biosym package[22] on a Silicon-Graphics computer. The X-ray structures of **1** were used to build the molecular structure and topology for **2–3**, with removal conversion of the 2' hydroxy group of the desosamine sugar modified in an acylated functional group. The starting coordinates of erythromycin (**1**) are used as the starting conformation for the simulation of the metabolite **4** with removal conversion of the 6 and 11-hydroxyl groups and the lactone group by a 6,9;9,12-spiroketal. The starting structures of the molecules **4** presents the disadvantage of not being based on X-ray information. The technique used for generating the structures **4–7** included simulated-annealing and conformational systematic searches by rotation of torsion angles.[8] The macrocycle was fixed in the **B2** geometry as also found by NMR in the solution-state conformation, the motion of erythronolide being very restricted.

To simulate the molecular movements in solution, different protocols were used. Recently, the computational methodologies[23] have illustrated the usefulness of MD in investigating possible conformations in solution. The structural information (dihedral angles and spatial proximity) of the different conformations generated in a previous study[8] would be of great benefit as references in predicting the conformation in solution of these new derivatives.

For an exploration of the conformational space, after an equilibration period of 4 ps, the dynamics are run at 300 K with periodical jumps at 600 K to supply the system with energy (in order to pass conformational barriers). The 42 ps trajectory is sampled every picosecond, the structures are then minimized by molecular mechanics and stored.

We have run experiments starting from each one of the possible conformations to compare their energies in case the interconversion was not observed.

A widely used method to mimic the screening effect of the solvent is to use a distance-dependent dielectric constant $\varepsilon = r$, leading to an r^2 dependence of the coulombic energy.[24] Use of a distance-dependent dielectric constant ($\varepsilon = r$) in the absence of explicit solvent is common. We applied it to each one of the possible conformations. The stability of the different conformers has been tested by a 100 ps dynamics protocol at 300 K. All the dihedral angles measured varied less than 10° during the dynamics, except for the desosamine sugar which exchanges its positions **a**, **b** and **c** by 40–90° rotation around the glycosidic bonds.

The ratio of **b** to **c** conformers observed statistically during a 100 ps dynamics protocol, agrees with the ratio calculated (Table 5) by the Boltzmann distribution of **1–6** but it is inversed for **7**. The above calculations presumed the default value of $\varepsilon = r$ for the local dielectric constant, a reasonable analogy for the solvent in spite of the uncertainty regarding a parameter considering or ignoring the rotational entropy of the plane of aromatic rings.

During the MD simulation of erythromycin derivatives **1–3**, the three structures named **A1a**, **A1c** and **B1b** were in conformational equilibrium with a major participation of the more stable conformer **A1a** (Fig. 3).

The energies of the **a**, **b** and **c** conformers were compared and the difference between **a** and **b** is not very significant (≈ 2 kcal mol^{-1}). Only one conformer of the erythronolide ring **A1a** (Fig. 3), is presumed potentially stable for benzoylated erythromycin **3**. This is coherent with the NMR results, confirming that the **Aa** conformer is the dominant one in solution. For erythromycin (**1**), and its propionate derivative **2**, the **Aa** structures are stable during the whole protocol (43–44%) with only a change of 3-4% of the **Bb** and **Ac** forms.

If we examine the chemical shift values (at the concentration 10^{-3} mol dm^{-3}) for protons of OH groups (Table 2), we notice the high-frequency shift for the OH(6) proton in **2** and **3** by comparison with that of **1**. In contrast, we observe a shift of the OH(11) and (12) signals to lower frequency. So, in the esterified erythromycin derivatives, OH(6) is more implicated in hydrogen bonding than OH(11) and (12). The 2'-OR strengthens the rigidification of the erythronolide region C(3)–C(7) and the hydrogen bond involving OH(6). Consequently the degree of movement of the desosamine and the cladinose sugar decreases in the following ways. In the esterified erythromycin **3** the benzoyl ring is situated close to the desosamine sugar. This sugar is thus pushed back on the cladinose (their two α faces are opposite to each other), and the desosamine enclosed between these two planes of the rings consequently loses some of its mobility.

During the MD simulation of erythralosamine (**4**), the **B2b** conformer was the major structure for this metabolite with the remaining **B2c** and **B2e** minor conformations (Fig. 4) corresponding to structures of higher energy (1–3 kcal mol^{-1} above the global minimum) (Table 5). For the molecule **4**, the locking on these torsion angles implies no possibility of interconversion with any **A** conformation, thus only one rigid conformation **B2** is observed. But the amplitude of movement of the ethyl group C(14)–C(15) leads to two positions, parallel and perpendicular to the macrocycle, only for the conformations **b** and **c** (9 and 2% respectively).

The MD simulation of erythralosamine derivatives **5–7**, reveals that the **B2** conformer remains the major

structure with the possible **b** and **c** sugar ring conformations. Rotation around the glycosidic bonds leading to the minor conformer **e** becomes sterically unfavourable with esterification. The most significative dihedral angles of the minima for **b** and **c** were measured and compared to the values of conformer in solution according to NMR results (Tables 4 and 5). Obviously, the values for **b** are very close to the NMR data.

For **5**, two conformers are possible that correspond to NMR results (Fig. 4). In the first conformer **B2b** the benzoyl group adopts an orientation nearly perpendicular to the macrocycle lactone ring (like the cladinose sugar in erythromycin). The desosamine sugar displays the same tendency to tilt up, whereas the two units appear to be in the same plane in conformation **B2c**. The energies of **b** and **c** are in the same range separated by only 0.1 kcal mol^{-1}, thus these conformers should readily interconvert at room temperature. In the compound **5**, the benzoyl ring in position C(3) induces the same steric hindrance as that of the cladinose ring facing the desosamine sugar in erythromycin A.

The other compound **6** benzoylated in the 2'-position has also two sugar conformers **b** and **c** with the ethyl group C(14)–C(15) leading to the two positions, parallel and perpendicular to the macrocycle (11 and 2% respectively). At 300 K, the conformation **b**, predominant in solution according to NMR results, has energy about 2 kcal lower than the **c** conformer (Fig. 4). Conformer **b** with the Me(15) group parallel to the Me(2), corresponds to the global minimum energy conformation. However, in contrast with the 3-benzoate, the other conformer **c** is not at all energetically similar to the global minimum. An unfavourable steric interaction between the macrocycle and the coplanar sugar ring (with the aromatic ring moving down perpendicularly) raises the energy. Thus, the lowest energy conformers of **b** and **c** are separated by as much as 2 kcal mol^{-1}. In contrast with its isomer **5**, the compound **6** is predicted to be locked in the **B2b** conformation at room temperature. At 300 K, the conformation **b** is predominant in solution according to NMR data.

For the 2',3-dibenzoate derivative **7**, the greater proportion of a conformer **B2c** is predicted (Fig. 4). The 2'-benzoyl group is more stabilized for **7** due to greater proximity to the other parallel aromatic ring than in the **c** conformers **5** or **6**. The spatial relationship between the aromatic π electrons was defined in terms of attractive potential between the ring planes at a definite distance on the axis from the two ring centres. Thus, presuming a Boltzmann distribution of **7** over the two conformations **b** and **c**, which differ in energy by $\Delta E = 1.8$ kcal mol^{-1}, the population of the higher energy conformer **b** would change from 75% in **6** to 15% in **7**.

Structure–activity analysis

Studies of the biological properties[1-3] of the macrolide antibiotics reveal higher affinity with the cytochrome P450 for erythralosamine compared to erythromycin. It could thus be stated that the conformer **b** with a lift up orientation of the desosamine sugar may be the active form interacting with the hemoprotein. The slight participation of the **e** form for erythralosamine could involve it as a potent active form. Determination of the heteronuclear coupling constants for glycosidic bonds revealed that interconversion of type **b** and **c** is both allowed and observed, for the metabolite series **4–7**.

For benzoylated erythromycin **3**, the **Aa** conformer is the preponderant one in solution (Fig. 3), that is coherent with the MD and NMR results, and at the same time, this 2'-benzoate derivative does not produce stable cytochrome Fe(II)–RNO complexes both *in vivo* and *in vitro*[5,6] (Fig. 1). For erythromycin (**1**), and its propionate derivative **2**, the **Aa** structures are stable during the whole protocol with only a variation of per cent amount of the **Bb** and **Ac** forms. Similarly, the 2'-propionate biological activity revealed that small amounts P450–metabolite complex were formed, slightly better than **1** (Fig. 1).

For **5**, two conformers of energy in the same range are possible, that correspond to NMR results (Fig. 4). In the first conformer **B2b** the benzoyl group adopts an orientation nearly similar to that of the cladinose sugar in erythromycin. The desosamine sugar displays the same tendency to tilt up, whereas the two units appear to be in the same plane in conformation **B2c**. Concerning formation of the cytochrome Fe(II)–RNO complex, an important decreasing (by 50%) of the complex is observed perhaps related to the increase of conformation **c** in **5** with respect to conformation **b** in **4**. In the compound **5**, the benzoyl ring in position C(3) induces the same steric hindrance as that of the cladinose ring facing the desosamine sugar in erythromycin A. Thus, we find for this derivative, an intermediate biological activity situated between erythralosamine (its parent molecule) and erythromycin A.

The other compound **6** benzoylated in the 2'-position leads to the two sugar positions, parallel and perpendicular to the macrocycle. The conformation **b** is predominant in solution according to NMR data, and at the same time, the formation of the cytochrome P450 Fe(II)–RNO complex is three to four times higher than for its parent product, erythralosamine (**4**) (Fig. 1).

For the 2',3-dibenzoate derivative **7**, the greater proportion of a conformer **B2c** is predicted (Fig. 4) as the 2'-benzoyl group is more stabilized by the stacking of the parallel aromatic ring planes. It is important to note that **7** is fully inactive for cytochrome P450 activity (Fig. 1).

As the 3'-dimethylamino function of the desosamine is responsible for the interaction with cytochrome P450, its position, mobility and the steric hindrance on the proximity of this functional group could be related to its biological properties. The desosamine group in the

erythromycin derivatives is found to be perpendicular (**a** conformer) while both sugar groups are parallel in order to reduce the steric energy. In the erythralosamine derivatives the steric parameters favour the **b** conformers in which the amino group is tilted up, while only in one case (in particular 2',3-dibenzoylated **7**) the stacking aromatic attraction stabilizes the planar **c** conformer.

Both isomers **b** and **c** are thus shown to adopt well-defined conformations and prove to be well-adapted for comparative structure–activity correlation studies. Accordingly, the amounts of metabolite complex (Fig. 1) increase in the order of compounds **3** < **7** < **1** < **2** < **5** < **4** < **6**, almost in parallel with the increase of the conformer's ratio **b/c** (Fig. 4).

There is an exception in the case of **7** with 15% **b** versus **2** with 5% **b**, however **2** forms small amounts of complex while **7** does not. Perhaps there are a number of explanations which tend to clarify this deviation. The formation of the cytochrome Fe(II)–RNO complex depends on many factors, such as hydrophobicity, hindrance around the dimethyl-amino function, ionization state of the $N(CH_3)_2$ group,[7] a series of multiple steps of metabolism of the $N(CH_3)_2$ group into nitrosoalkane reactive species (RNO), and these factors may include conformation in solution. Also the standard error mean values concerning low amounts of complex formation are often in the range of 10%. Hence, for a small percentage of **b** conformation, the structure–activity correlation is less reliable.

Conclusion

We have shown that the NMR data have been necessary to optimize the molecular dynamics protocol that now can be used directly and rapidly for the conformational analysis of other molecules, of a similarly limited size, within the same family of antibiotics. NMR data confirm some of the conclusions mentioned in the previous section. It has been shown that these molecules could be present in several conformers in solution. Erythromycin (**1**) possesses a lactone ring reorganized in the C(3)–C(5) region in the models **A** and **B**, but this slight **B** participation decreases for its acylated derivatives **2** and **3**. The minor conformation **B** with a sugar ring **b** lifted up above the macrocycle increases significantly for its metabolite series **4**–**7**. For erythralosamine benzoylated derivative **6**, obviously, the data are compatible with the conformation model **b**. For the **5** compound, NMR and MD studies show that the benzoyl group attached in the 3-position of the macrolactone is parallel or coplanar to the desosamine sugar and masks the dimethylamino group by steric hindrance. This observation is detrimental for metabolite complex formation when compared to erythralosamine. This phenomenon is additionally amplified when both 2' and 3 positions are esterified as in compound **7**.

The biological activity of an erythromycin or erythralosamine derivative depends on many factors, and these may include its conformation in solution. The use of the NMR and MD data presented, offers an efficient method to estimate conformation of a new series of erythromycin derivatives in solution. By comparison with MD data for these compounds, an estimate of the solution conformation can be simply derived.

The desosamine group in the erythromycin derivatives is found to be perpendicular (**a** conformer) while in the erythralosamine derivatives the steric parameters favour the **b** conformers in which the amino group is tilted up. Only in one case (in particular 3,2'-dibenzoylated **7**) the stacking aromatic attraction stabilizes the planar **c** conformer.

Both isomers **b** and **c** are thus shown to adopt well-defined conformations and prove to be well-adapted for comparative structure–activity correlation studies (Fig. 4).

Experimental

NMR Spectroscopy

The samples were dissolved in $CDCl_3$ solution; the concentrations of 10^{-3} mol dm^{-3} for the ^1H experiments and 10^{-2} mol dm^{-3} for the ^{13}C experiments could be attained. Degassed and sealed tubes were used for the T_1 determinations and ^1H NOESY experiment.

The experiments were run at 250 and 500 MHz for ^1H, and 62.9 MHz for ^{13}C, on Bruker WM 250 and AMX 500 spectrometers, at room temperature.

The DEPT polarization transfer from ^1H to ^{13}C nuclei with decoupled spectra, the 2D ^1H, ^1H COSY spectra, the 2D ^1H, ^{13}C COSY experiments, the homonuclear *J*-resolved 2D NMR experiments using the Hahn spin-echo, the ^{13}C T_1 relaxation time measurements using an inversion–recovery pulse sequence, the 2D phase sensitive ^1H NOESY using for the mixing time (D8) (D9 P2 A0) instead of a variable delay D9 and the measurement of long-range heteronuclear ^3J ^{13}C–^1H coupling constants were described in previous studies.[8,19,23]

Molecular dynamics

The calculations were run on a Silicon Graphics computer using the Biosym software INSIGHT II and 'DISCOVER'.

The structures were derived from the crystallographic coordinates of the solid **1** as a starting point and the substituents were modified. For the molecular dynamics calculations, the trajectories were calculated thanks to the Verlet Algorithm used in the force-field of DISCOVER. The starting structures were first

minimized using 500 steps of the "Steepest Descent" algorithm and then the "Conjugate Gradients" algorithm until a convergence of 0.1 kcal mol^{-1} was reached.

The system was then equilibrated during a period of 4 ps to reach a temperature of 300 K by coupling it to a thermal bath.[25] The dynamics were run for 42 ps (variable temperature, 600 K/300 K) or 100 ps (constant temperature, 300 K) and the trajectory was sampled by minimizing and storing the structure every picosecond so that 100 conformations were recorded by the end of the MD simulation. Detailed protocol and analysis are not provided here but are referred to previous work.[23]

For the electrostatic energies, since no explicit solvent molecules were incorporated during the run, the dielectric constant was set distance-dependent ($\varepsilon = R_{ij}$), to mimic the solvent effect.

Coupling constants were calculated from the torsion angles using the Altona software on a Macintosh II computer.

Acknowledgements

We would like to thank Dr J. Belanger for technical help. We thank Laboratoire Roussel (Paris) for their scientific and financial support during this research.

References

1. Kirst, H. A. *Ann. Rep. Med. Chem.* **1989**, *25*, 119.

2. Sakakibara, H.; Okekawa, O.; Fujiwara, T.; Otani, M.; Omura, S. *J. Antibiot.* **1981**, *34*, 1001.

3. Martin, Y. C.; Jones, P. H.; Perun, T. J.; Grundy, W. E.; Bell, S.; Bower, R. R.; Shipkowitz, N. L. *J. Med. Chem.* **1972**, *15*, 635.

4. Delaforge, M.; Sartori, E.; Mansuy, D. *Chem.- Biol. Inter.* **1988**, *68*, 179.

5. Sartori, E.; Delaforge, M.; Mansuy, D. *Biochem. Pharm.* **1989**, *38*, 2061.

6. Delaforge, M.; Sartori, E. *Biochem. Pharm.* **1990**, *40*, 223.

7. Delaforge, M.; Ladam, P.; Bouillé, G.; Gharbi-Benarous, J.; Jaouen, M.; Girault, J. P. *Chem.- Biol. Inter.* **1992**, *85*, 215.

8. Gharbi-Benarous, J.; Ladam, P.; Delaforge, M.; Girault, J. P. *J. Chem. Soc. Perkin Trans. 2* **1993**, 2303.

9. (a) Everett, J. R.; Tyler, J. W. *J. Chem. Soc. Perkin Trans. 2* **1987**, 1659; *ibid.* **1988**, 325; (b) Everett, J. R.; Tyler, J. W. *J. Chem. Soc., Chem. Commun.* **1987**, 815; (c) Everett, J. R.; Tyler, J. W. *Magn. Reson. in Chem.* **1988**, *26*, 179.

10. Nakagawa, A.; Omura, S. *Macrolide Antibiotics. Chemistry, Biology, and Practice,* Omura, S. Ed.; Academic Press; Orlando, 1984.

11. Mulzer, J.; Kirstein, H. M.; Buschmann, J.; Lehmann, C.; Luger, P. *J. Am. Chem. Soc.* **1991**, *113*, 910.

12. Egan, R. S.; Perun, T. J.; Martin, J. R.; Mitscher, L. A. *Tetrahedron* **1973**, *29*, 2525; Perun, T. J.; Egan, R. S.; Martin, J. R. *Tetrahedron Lett.* **1969**, 4501.

13. Harris, D. R.; Mc Geachin, S. G.; Mills, H. H. *Tetrahedron Lett.* **1965**, 679.

14. Bendall, M. R.; Pegg D. T. *J. Magn. Reson.* **1983**, *53*, 272.

15. Bax, A.; Freeman, R. *J. Magn. Reson.* **1981**, *44*, 542.

16. Rutar, J. A. *J. Magn. Reson.* **1984**, *59*, 306; Wong, T. C.; Rutar, V. *J. Am. Chem. Soc.* **1984**, *106*, 7380.

17. (a) Altona, C.; Sudaralingam, M. *J. Am. Chem. Soc.* **1973**, *95*, 2333; (b) Haasnoot, C. A. G.; de Leeuw, F. A. A. M.; Altona, C. *Tetrahedron* **1980**, *36*, 2783.

18. Tvaroska, I.; Hricovini, M.; Petrakova, E. *Carbohydr. Res.* **1989**, *189*, 359.

19. (a) Ladam, P.; Gharbi-Benarous, J.; Pioto, M.; Delaforge, M.; Girault, J. P. *Magn. Reson. in Chem.* **1994**, *32*, 1; (b) Jippo, T.; Kamo, O.; Nagayama, K. *J. Magn. Reson.* **1986**, *66*, 344.

20. Marion, D.; Wuthrich, K. *Biochem. Biophys. Res. Commun.* **1983**, *113*, 976.

21. Allerhand, A.; Doddrell, D.; Komoroski, R. *J. Chem. Phys.* **1971**, *55*, 189; Lyerla, J. R.; Levy, G. C. *Top. Carbon-13 NMR Spectrosc.* **1974**, *1*, 79.

22. Dauber-Osguthorpe, P.; Roberts, V. A.; Osguthorpe, D. J.; Wolff, J.; Genest, M.; Hagler, A. T. *Proteins: Structure, Function and Genetics.* **1988**, *4*, 31.

23. Gharbi-Benarous, J.; Ladam, P.; Delaforge, M.; Girault, J. P. *J. Chem. Soc. Perkin Trans. 2* **1992**, 1989.

24. Burt, S. K.; Mackay, D.; Hagler, A. T. *Computer-Aided Drug Design*, p. 66, Perun, T. J.; Propst C. L., Eds; Marcel Dekker, Inc.; New York, 1989.

25. Berendsen, H. J. C.; Postma, J. P. M.; Van Gunsteren, W. F.; DiNola, A.; Haak, J. R. *J. Chem. Phys.* **1984**, *81*, 3684.

(*Received in U.S.A.* 8 *November* 1994; *accepted* 27 *February* 1995)

Supplementary Material

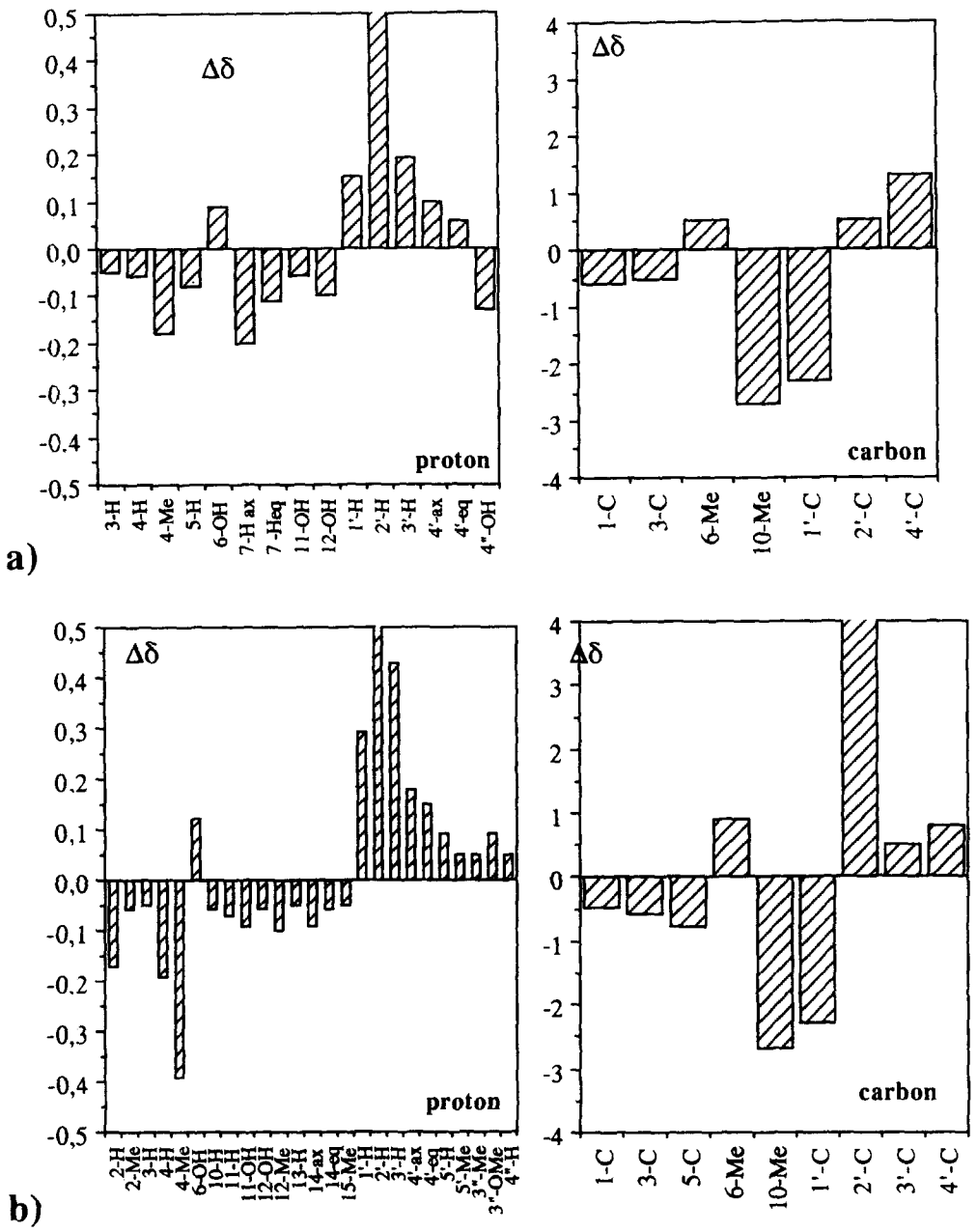

Figure S1. Differences of ^{1}H and ^{13}C chemical shifts between (**a**) erythromycin A (**1**) and 2'-propionate erythromycin (**2**); (**b**) erythromycin A (**1**) and 2'-benzoate erythromycin (**3**).

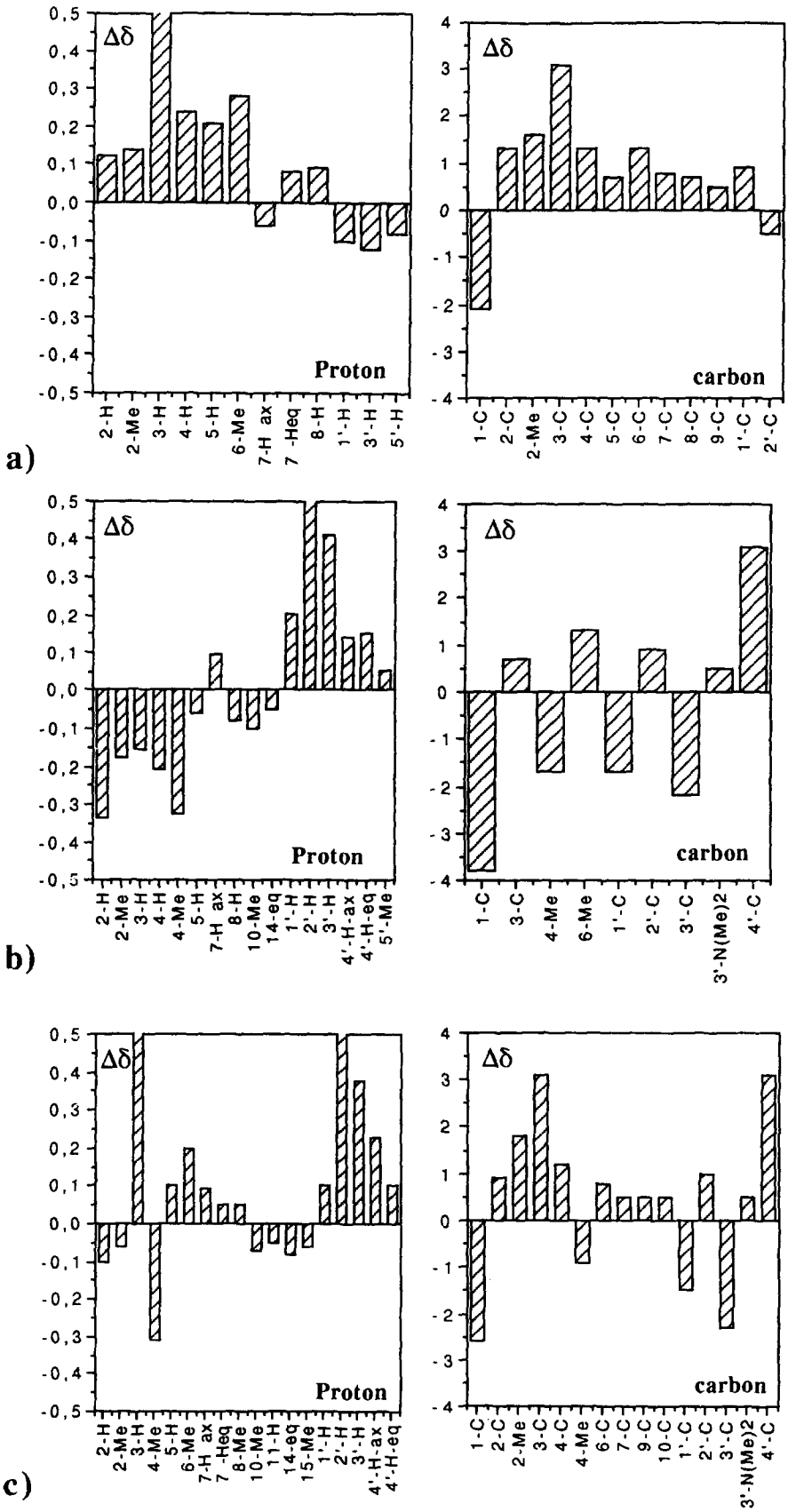

Figure S2. Differences of ^{1}H and ^{13}C chemical shifts between (**a**) erythralosamine (**4**) and 3-benzoate erythralosamine (**5**); (**b**) erythralosamine (**4**) and 2'-benzoate erythralosamine (**6**); (**c**) erythralosamine (**4**) and 3,2'-dibenzoate erythralosamine (**7**).